Journal of Molecular Spectroscopy **204,** 216–225 (2000)
doi:10.1006/jmsp.2000.8221, available online at http://www.idealibrary.com on IDEAL®

High-Resolution Study of the ($\nu_1 + \frac{1}{2}\nu_2 + \nu_3 = 3$) Polyad of Strongly Interacting Vibrational Bands of D_2O

O. N. Ulenikov,* Sheng-Gui He,† G. A. Onopenko,* E. S. Bekhtereva,* Xiang-Huai Wang,† Shui-Ming Hu,† Hai Lin,† and Qing-Shi Zhu†

*Laboratory of Molecular Spectroscopy, Physics Department, Tomsk State University, Tomsk, 634050, Russia; and †Open Laboratory of Bond-Selective Chemistry and High Institute for Advanced Research, University of Science and Thechnology of China, Hefei, 230026 People's Republic of China

Received May 8, 2000; in revised form July 19, 2000

Analysis of the high-resolution Fourier transform spectra of the D_2O first decade was carried out in the framework of the Hamiltonian model which took into account resonance interactions between the seven states, (300), (201), (102), (003), (220), (121), and (022). Assigned from the experimentally recorded spectrum transitions belonged to the four bands, $2\nu_1 + \nu_3$, $3\nu_3$, $\nu_1 + 2\nu_2 + \nu_3$, and $3\nu_1$, gave the possibility both of obtaining rotational, centrifugal distortion, and resonance interaction parameters of "appeared" states, (201), (003), (121), and (300), and of estimating from the fit band centers, rotational, and resonance interaction parameters of the three "dark" states, (220), (022), and (102). © 2000 Academic Press

1. INTRODUCTION

In recent contributions (*1–2*) we discussed results of the study of high-resolution Fourier transform spectra of the D_2O molecule in the regions of location of the ($\nu_1 + \frac{1}{2}\nu_2 + \nu_3 = \frac{3}{2}$) and ($\nu_1 + \frac{1}{2}\nu_2 + \nu_3 = 2$) poliads (the short review of the earlier studies of the D_2O spectra can be found in (*1*)). The present study, being the continuation of those analyses, is devoted to the investigation of high-resolution spectrum of the next ($\nu_1 + \frac{1}{2}\nu_2 + \nu_3 = 3$) poliad of the D_2O molecule which is mostly located in the region 7500–8300 cm^{-1}.

Earlier, spectra of the D_2O molecule in this region were mentioned only in two papers, Refs. (*3–4*), by the strongest $2\nu_1 + \nu_3$ band. In our case, spectra belonging to the $2\nu_1 + \nu_3$, $3\nu_3$, $\nu_1 + 2\nu_2 + \nu_3$, and $3\nu_1$ vibration–rotation bands were recorded and analyzed. Experimental details and the Hamiltonian model further used in the analysis of the recorded spectrum are described in Sections 2 and 3, respectively. Sections 4 and 5 present results of assignments of spectral lines and analysis of results, respectively.

2. EXPERIMENTAL DETAILS

The sample of D_2O was purchased from PeKing Chemical Industry, Ltd. (China). The stated abundance of deuterium was 99.8%. The spectra were recorded at room temperature with a Bruker IFS 120HR Fourier transform spectrometer (Hefei), which was equipped with a multipass gas cell with adjustable path length, a tungsten source, a CaF_2 beamsplitter, and a Ge diode detector. The unapodized resolution was 0.01 cm^{-1}, and the apodization function was the boxcar.

Since the H_2O and the HDO molecules also absorb in the region 7500–8500 cm^{-1}, where the studied bands of the D_2O are located, the same method, as in our recent contributions (*1–2*), was used. Namely, we measured two spectra with different ratios of D_2O to HDO and H_2O in the sample. The first spectrum was recorded at a total pressure of 1500 Pa with the percentage of D_2O being approximately 75% and the path length being 69 m. The corresponding conditions for the second spectrum were 1090 Pa, 25%, and 15 m, respectively. The signal-to-noise ratio was estimated as about 400 for the first spectrum and 360 for the second spectrum. The line positions were calibrated with those of the H_2O from the HITRAN96 data base. For illustration, some fragments of the recorded spectra are presented in Figs. 1–4.

3. HAMILTONIAN MODEL

The ($\nu_1 + \frac{1}{2}\nu_2 + \nu_3 = 3$) poliad consists of 10 interacting vibrational states (300), (201), (102), (003), (220), (121), (022), (140), (041), and (060). However, we found that to describe the rovibrational energies determined in the current study from experimental data it is not necessary to take into account influence of the states (140), (041), and (060). At the same time, the states (300), (201), (102), and (003) strongly interact with each other and are perturbed by the (220), (121), and (022) states. Really, as was mentioned in the introduction, we were able to assigned lines belonging to the four vibration–rotation bands, $2\nu_1 + \nu_3$, $3\nu_3$, $3\nu_1$, and $\nu_1 + 2\nu_2 + \nu_3$. This means that the three last states of the poliad, (140), (041), and (060), practically do not exert influence on the values discussed in the current contribution vibration–rotation energies of the (300), (201), (102), and (003) states and can perturb only the energies of the (121) state. However, as further analysis showed, the last effect can be neglected in our study also (at least, we preferred to sacrifice by taking into account possibly two- to three additional vibration–rotation states of the

0022-2852/00 $35.00

TABLE 1
Statistical Information on Bands of the D_2O Molecule (First Decade)

Band	Band center, our in cm^{-1}	Band center, (δ) in cm^{-1}	J^{max}	K_a^{max}	Number of lines	Number of upper energies	n_1[a]	n_2[a]	n_3[a]
1	2	3	4	5	6	7	8	9	10
$3\nu_1$	7852.928	7859.5	10	4	202	57	19	15	23
$2\nu_1 + \nu_3$	7899.825	7905.1	14	7	384	127	60	43	24
$\nu_1 + 2\nu_3$	8054.19	8057.2							
$3\nu_3$	8220.178	8220.9	12	7	278	111	57	32	22
$2\nu_1 + 2\nu_2$	7593.08	7591.5							
$\nu_1 + 2\nu_2 + \nu_3$	7672.923	7671.9	11	6	196	62	18	17	27
$2\nu_2 + 2\nu_3$	7825.395	7824.7	8	4	6	2	2	-	-

[a] n_1, n_2, and n_3 in columns 8, 9, and 10 are the numbers of energies of upper vibrational states which are reproduced by the excited state parameters within the accuracies: n_1 $0 \le |\delta| \le 0.002$ cm^{-1}; n_2 $0.002 \le |\delta| \le 0.005$ cm^{-1}, and n_3 $0.005 \le |\delta|$ cm^{-1}, respectively.

(121) state, which can be perturbed by the (140) or (041) states, for reduction of the number of vibrational states used in the model). To resume, the Hamiltonian which was used in our present analysis took into account seven interacting vibrational states and had the form[1]

$$H^{\text{eff}} = \sum_{i,j} |i\rangle\langle j| H^{ij}, \qquad [1]$$

where $i, j = 1$–7, and the following notations are used: $|1\rangle =$ (300), $|2\rangle =$ (102), $|3\rangle =$ (220), $|4\rangle =$ (022), $|5\rangle =$ (201), $|6\rangle =$ (003), and $|7\rangle =$ (121). "Diagonal" operators H^{ii} ($i = 1, 2, 3, 4, 5, 6, 7$) are the usual Watson's operators (5):

$$\begin{aligned} H^{ii} = {} & E^i + [A^i - \tfrac{1}{2}(B^i + C^i)]J_z^2 + \tfrac{1}{2}(B^i + C^i)J^2 \\ & + \tfrac{1}{2}(B^i - C^i)J_{xy}^2 - \Delta_K^i J_z^4 - \Delta_{JK}^i J_z^2 J^2 \\ & - \Delta_J^i J^4 - \delta_K^i [J_z^2, J_{xy}^2] - 2\delta_J^i J^2 J_{xy}^2 \\ & + H_K^i J_z^6 + H_{KJ}^i J_z^4 J^2 + H_{JK}^i J_z^2 J^4 + H_J^i J^6 \\ & + [J_{xy}^2, h_K^i J_z^4 + h_{JK}^i J^2 J_z^2 + h_J^i J^4] + L_K^i J_z^8 \\ & + L_{KJK}^i J_z^6 J^2 + L_{KJ}^i J_z^4 J^4 + L_{JJK}^I J_z^6 J^2 + L_J^i J^8 \\ & + [J_{xy}^2, l_K^i J_z^6 + l_J^i J^6] + P_K^i J_z^{10}. \end{aligned} \qquad [2]$$

[1] One should expect that an appearance of experimental rovibrational energies with higher values of the quantum numbers J and K_a than in our present study will sooner or later lead to the necessity of taking into account the resonance interactions with the states (140), (041), and (060) also.

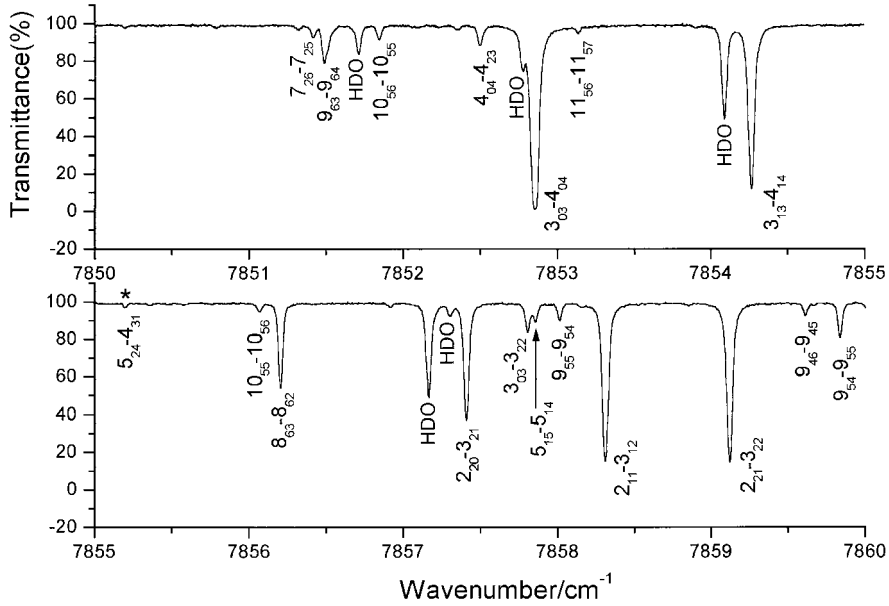

FIG. 1. A small part of the D_2O spectra showing line assignments in the strongest $2\nu_1 + \nu_3$ band. The spectrum was measured at the pressure of 1500 Pa (about 75% of D_2O, 15% of HDO, and 10% of H_2O), with the absorption path length of 69 m. Lines marked with H are originated from the HDO absorption in the sample. One line, marked by *, belongs to the $3\nu_1$ band.

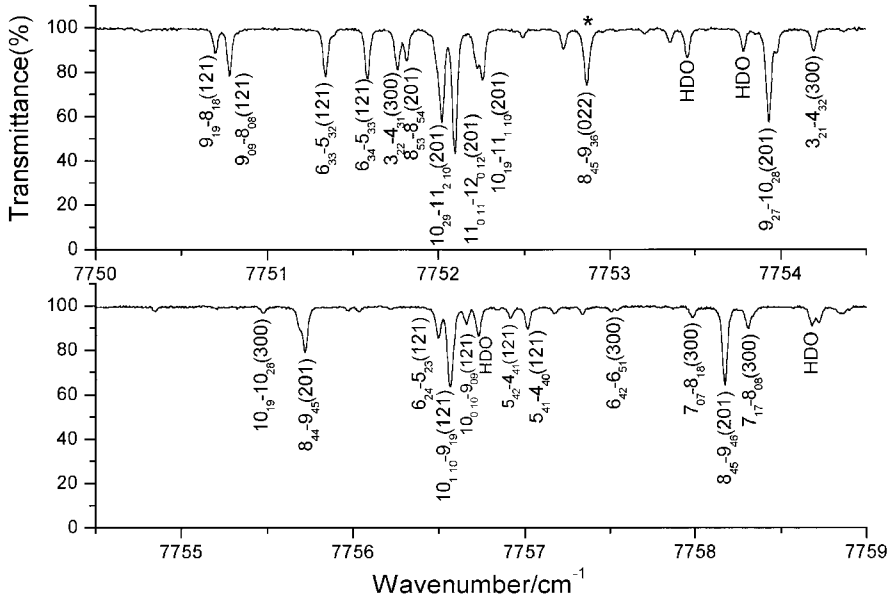

FIG. 2. A small part of the region of location of the weak $3\nu_1$ band. Some strong P-branch lines of the $2\nu_1 + \nu_3$ band can be seen also. The experimental conditions are the same as in Fig. 1. One of six lines assigned to the $2\nu_2 + 2\nu_3$ band (it is marked by *) can be seen also.

The $H^{ij} = H^{ji+}$ $(i \neq j)$ are operators of different kinds of resonance interactions. In this case, the operators H_{ij}, which describe interactions between the states of the same symmetries, have the form:

$$\begin{aligned} H^{ij} = H^{ji+} = {} & F_0^{ij} + F_K^{ij} J_z^2 + \cdots \\ & + F_{xy}^{ij} J_{xy}^2 + F_{xyK}^{ij} [J_{xy}^2, J_z^2]_+ \\ & + F_{xyJ}^{ij} J_{xy}^2 J^2 + F_{xyKK}^{ij} [J_{xy}^2, J_z^4]_+ \cdots \end{aligned} \qquad [3]$$

In turn, the operators which describe interactions between the states of different symmetries (A_1 and B_1) have the form:

$$\begin{aligned} H^{ij} = H^{ji+} = {} & C_y^{ij} i J_y + C_{yK}^{ij} [i J_y, J_z^2]_+ C_{yJ}^{ij} i J_y J^2 \\ & + C_{yKK}^{ij} [i J_y, J_z^4]_+ \cdots + C_{xz}^{ij} [J_x, J_z]_+ \\ & + C_{xzK}^{ij} [[J_x, J_z]_+, J_z^2]_+ + C_{xzJ}^{ij} [J_x, J_z]_+ J^2 \cdots \\ & + C_{xzKK}^{ij} [[J_x, J_z]_+, J_z^4]_+ \end{aligned}$$

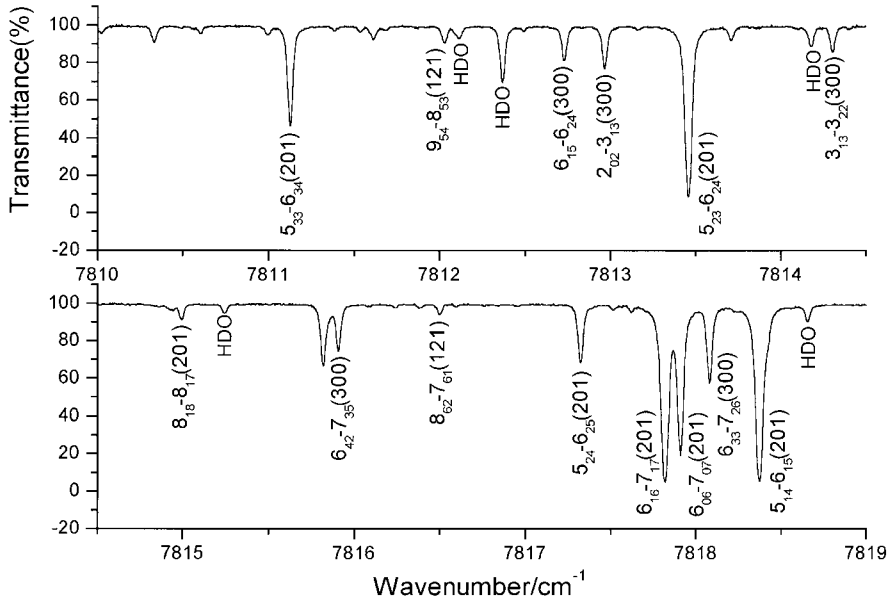

FIG. 3. Part of the spectrum showing line assignments for the blended region of the $\nu_1 + 2\nu_2 + \nu_3$, $2\nu_1 + \nu_3$, and $3\nu_1$ bands. The experimental conditions are the same as in Fig. 1.

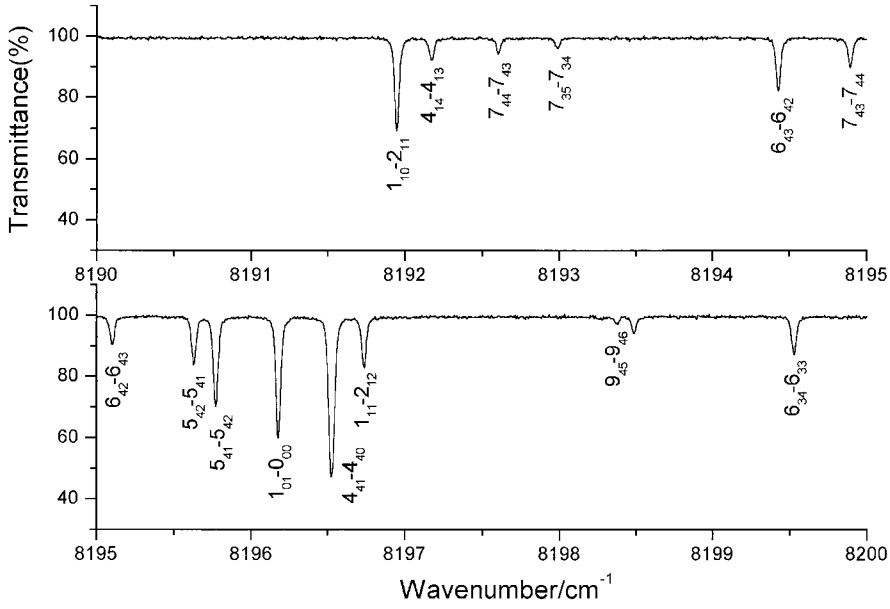

FIG. 4. Part of the spectrum in the region where the $3\nu_3$ band is located. For the experimental conditions, see Fig. 1.

$$+ C^{ij}_{xzJK}[[J_x, J_z]_+, J_z^2]_+ J^2 + \cdots$$
$$+ C^{ij}_{yxy}[J_y, J_{xy}]_+ + C^{ij}_{yxyK}[[J_y, J_{xy}]_+, J_z^2]_+ \cdots . \quad [4]$$

In Eqs. [2]–[4] the following notations are used: $J_{xy}^2 = J_x^2 - J_y^2$ and $J^2 = \Sigma_\alpha J_\alpha^2$.

As for the first hexad (*2*), the analysis studied in the present bands shows that their rovibrational energies cannot be reproduced with satisfactory accuracy if we do not take into account extra resonance interaction of the $(v_1v_2v_3) - (v_1 \mp 2v_2 \pm 2v_3 \pm 1)$ type which is different from the usual Fermi, Darling–Dannison, and Coriolis interactions (its nature was discussed in detail in Ref. (*2*)). In the present study interactions between the pairs of the states (201) and (022), (300) and (121), respectively, are described. One more interaction [in our case, it is the weak Fermi-type interaction between the states (300) and (022)] should be mentioned also. It originated from the

$$\langle k_{133} q_1 q_3^2 \rangle \langle k_{1122} q_1^2 q_2^2 \rangle \left[\frac{1}{2\omega_3 - \omega_1} + \frac{1}{2(\omega_1 - \omega_2)} \right] \quad [5]$$

-type terms in the effective vibration–rotation operator (see (*2*) for more details) and, in accordance with the general principles of the vibration–rotation theory (*6*), should be the value on the order of 5–20 cm^{-1}. If taking into account that the difference between the E^{300} and E^{022} vibrational energies is about 100 cm^{-1} only (see Table 4 below), it is clear that the resonance interaction between the states (300) and (022) can occur.

4. ASSIGNMENTS OF TRANSITIONS

As was mentioned in the introduction, earlier transitions of the poliad studied in the present poliad were assigned to the $2\nu_1 + \nu_3$ band only (*3–4*). In our case, thanks to the high sensitivity of the spectrometer and the possibility of using long

TABLE 2
List of Transitions Belonging to the $2\nu_2 + 2\nu_3$ Band of D_2O

Upper			Lower			Line position,	Transmit.,	Upper energy,	Mean value,
J'	K'_a	K'_c	J	K_a	K_c	in cm^{-1}	in per cent	in cm^{-1}	in cm^{-1}
	1			2		3	4	5	6
4	4	0	3	3	1	7958.913	90.7	8115.518	8115.519
			5	3	3	7847.989	23.7	8115.519	
8	4	5	7	1	6	8048.231	96.7	8412.279	8412.281
			7	3	4	7976.220	57.9	8412.280	
			9	3	6	7752.867	74.0	8412.283	
			9	5	4	7629.013	97.4	8412.281	

TABLE 3

Experimental Rovibrational Term Values for the (300), (201), (003), and (121) Vibrational States of the D_2O Molecule (in cm^{-1})[a]

			(300)			(201)			(003)			(121)		
J	K_a	K_c	E	Δ	δ	E	Δ	δ	E	Δ	δ	E	Δ	δ
	1		2	3	4	5	6	7	8	9	10	11	12	13
0	0	0	7852.928		0				8220.178		2	7672.933		-10
1	0	1	7864.603	1	0	7911.571	1	0	8232.055	1	1	7684.844	1	-8
1	1	1	7872.230	3	-4	7918.898	1	-2	8238.805	2	0	7694.594	1	-1
1	1	0	7874.617	2	-2	7921.319	1	-8	8241.288	1	0	7697.275	1	-2
2	0	2	7887.475	1	4	7934.544	1	0	8255.237	0	3	7708.195	1	-5
2	1	2	7893.181	3	-6	7940.058	1	-2	8260.083	1	-1	7715.775	1	-4
2	1	1	7900.334	1	2	7947.280	1	2	8267.526	2	2	7723.809	2	-3
2	2	1	7923.106	2	-3	7969.154	1	-6	8287.706	1	-5	7752.861	1	8
2	2	0	7923.545	2	-2	7969.661	1	0	8288.275	2	-4	7753.340	2	6
3	0	3	7920.695	2	5	7967.841	1	-1	8288.749	1	3	7742.094	1	1
3	1	3	7924.342	4	-2	7971.577	1	-2	8291.666	1	0	7747.263	1	-6
3	1	2	7938.558	2	8	7985.794	2	3	8306.446	1	3	7763.238	2	-3
3	2	2	7958.040	2	-1	8006.104	1	5	8323.363	2	-4	7788.811	2	10
3	2	1	7960.081	3	-1	8007.870	1	4	8326.023	0	-1	7791.085	3	9
3	3	1	8001.189	2	10	8047.030	1	0	8363.278	2	-2	7843.432	1	-7
3	3	0	8000.612	1	7	8047.099	1	1	8363.361	1	-4	7843.487	0	-7
4	0	4	7963.434	1	5	8010.613	2	0	8331.749	0	8	7785.614	1	8
4	1	4	7965.454	5	2	8014.107	1	1	8333.261	1	-1	7788.804	1	-7
4	1	3	7988.789	2	9	8036.294	2	4	8357.427	2	6	7815.053	1	4
4	2	3	8004.265	2	-4	8046.768	2	-3	8370.419	2	-2	7836.325	1	3
4	2	2	8008.945	4	0	8058.748	1	1	8377.499	1	1	7842.533	2	7
4	3	2	8048.415	1	2	8093.811	1	0	8411.795	1	-4			
4	3	1	8054.315	1	-2	8094.256	2	-1	8412.362	1	-3			
4	4	1	8109.808	4	3	8152.897		4	8465.901		4	8042.804	4	2
4	4	0	8109.801	4	9	8152.905		5	8465.907	8	0			
5	0	5	8015.268	1	4	8062.472	1	-1	8383.907	1	1	7838.216	3	18
5	1	5	8016.269	3	0	8062.796	2	-2	8384.617	1	-2	7840.269	4	-8
5	1	4	8050.261	1	8	8097.939	1	8	8419.533	3	5	7878.478	1	2
5	2	4	8061.473	3	-4	8105.426	7	-3	8428.479	2	-3	7895.122	2	-7
5	2	3	8074.789	2	0	8122.724	1	-2	8442.579	1	3	7907.798	2	4
5	3	3	8107.979	3	-7	8152.516	1	0	8472.437	2	-5	7947.299	2	2
5	3	2	8114.401	4	-15	8154.120	2	2	8474.536	1	-1			
5	4	2	8170.444	2	-18	8211.792	1	-1	8526.754	2	0	8026.293	2	11
5	4	1	8170.353	2	-14	8211.842	1	-2	8526.844	1	0	8026.401	3	-8
5	5	1				8286.419	3	0	8595.297	3	16			
5	5	0				8286.419	3	4	8595.297	3	14			
6	0	6	8076.144	1	5	8123.407	2	-2	8445.233	1	0	7899.768	1	14
6	1	6	8076.604	3	-13	8123.586	2	-4	8445.580	1	-6	7899.745	0	0
6	1	5	8121.995	2	2	8169.690	1	5	8491.682	1	6	7952.491	2	-14
6	2	5	8129.291	3	-9	8173.486	1	-5	8497.129	2	-1	7965.026	4	-19
6	2	4	8151.004	2	-8	8199.500	2	0	8520.603	1	2	7986.491	2	1
6	3	4	8179.589	4	21	8223.088	4	3	8544.976	1	-2			
6	3	3	8187.349	2	-5	8227.197	1	7	8550.514	2	-1			
6	4	3	8243.470	2	1	8282.749	3	-4	8599.962	1	0	8098.536	2	-1
6	4	2	8243.106	5	15	8283.162	2	-2	8600.386	2	-1	8098.897	1	0
6	5	2				8357.248	1	-3	8668.465	4	7	8192.791	2	2
6	5	1				8357.154	1	-4	8668.465	4	-8	8192.791	2	2
6	6	1				8447.015	1	6	8750.937	2	5			
6	6	0				8447.015	1	6	8750.937	2	5			
7	0	7	8146.127	2	6	8193.496	2	-2	8515.810	0	0	7970.337	2	4
7	1	7	8146.328	3	3	8193.567	3	-4	8515.837	1	-5	7970.561	2	2
7	1	6				8250.665	1	1	8573.044	0	2	8036.129	2	4
7	2	6	8207.352	3	-8	8252.682	2	-2	8575.974	2	2	8046.818	2	14
7	2	5				8288.335	1	2	8610.652	1	1	8077.879	4	-5
7	3	5				8305.395	2	3	8629.052	1	0			

[a] In Table 3, Δ is the experimental uncertainty of the energy value, equal to one standard deviation in units of 10^{-3} cm^{-1}; δ is the difference $E^{exp} - E^{calc}$, also in units of 10^{-3} cm^{-1}; Δ is not quoted when the energy value was obtained from only one transition.

TABLE 3—*Continued*

			(300)			(201)			(003)			(121)		
J	K_a	K_c	E	Δ	δ	E	Δ	δ	E	Δ	δ	E	Δ	δ
	1		2	3	4	5	6	7	8	9	10	11	12	13
7	3	4				8313.533	2	-3	8640.587	2	1			
7	4	4	8329.199	1	15	8365.799	1	-3	8685.487	2	-2	8183.139	3	-2
7	4	3				8366.955	2	-3	8686.918	2	-3	8184.154	1	-9
7	5	3	8402.125	2	4	8439.442	2	-2	8753.983	5	-4	8277.246	5	7
7	5	2	8401.911	1	-6	8439.991	2	-1	8754.054	2	0	8277.246	5	-5
7	6	2				8529.445	3	-3	8836.604	2	2	8388.995	1	0
7	6	1				8529.445	3	-1	8836.604	2	1	8388.995	1	-1
7	7	1				8633.988	2	-3						
7	7	0				8633.988	2	-3						
8	0	8	8225.279	1	0	8272.787		-6	8595.706	0	1	8050.002	1	-6
8	1	8	8225.361	1	1	8272.817	2	4	8595.684	1	-1	8050.113	1	3
8	1	7	8293.055	2	4	8340.467	3	-2	8663.330	1	0	8128.658	2	5
8	2	7	8295.317	2	2	8341.408	1	-5	8664.690	1	1	8144.979	2	-3
8	2	6				8388.176	2	1	8711.618	1	-3			
8	3	6				8399.200	9	-4	8724.225	1	0			
8	3	5				8412.478	1	1	8744.389	2	3			
8	4	5	8428.134	1	-6	8460.877	2	-2	8783.182	2	-1			
8	4	4				8463.892	1	-2	8786.978	1	-4	8282.569	2	8
8	5	4				8534.394	1	3	8851.888	1	-1			
8	5	3				8535.083	1	1	8852.165	2	-4			
8	6	3				8623.925	3	-7	8934.575	5	2			
8	6	2				8623.925	3	5	8934.575	5	-9			
8	7	2				8728.039	4	2	9030.766	3	-11			
8	7	1				8728.039	4	6	9030.766	3	-11			
9	0	9				8361.315	3	-4	8685.023	1	4	8138.800		-21
9	1	9	8313.661	3	-16	8361.325	10	0	8684.910	1	0	8138.840		4
9	1	8				8439.095	2	-6	8762.632	1	-3	8229.878		6
9	2	8				8439.489	2	-3	8763.061	1	1			
9	2	7				8497.735	2	-5	8822.411	1	-6			
9	3	7				8503.950	2	1	8830.040	2	1			
9	3	6							8861.014	3	4			
9	4	6				8567.785	3	-4	8892.764	4	0			
9	4	5				8574.440	2	0	8901.083	4	-1			
9	5	5				8641.284	1	7	8962.150	3	-4			
9	5	4				8642.649	3	6	8963.038	3	-2			
9	6	4				8730.563	2	-3	9044.836	2	7			
9	6	3				8730.516	1	0	9044.881	1	6			
9	7	3							9141.610	2	5			
9	7	2							9141.610	2	4			
10	0	10	8411.159	4	10	8459.075	1	1	8784.731	3	8	8236.786		- 4
10	1	10	8411.172	1	-3	8459.084	2	10	8783.939	3	-4			
10	1	9				8546.691	2	-2	8871.250	4	-8	8339.843	2	- 1
10	2	9				8546.849	2	9	8870.980	3	5			
10	2	8				8619.361	1	-4	8942.356		-11			
10	3	8				8621.488	1	6	8946.084	1	1			
10	3	7				8643.841	1	0	8989.154	5	8			
10	4	7				8686.070	1	0	9013.849	2	2			
10	4	6				8698.721	1	-4	9029.347	2	-6			
10	5	6				8760.055	2	2	9084.680	3	-2			
10	5	5				8763.015	2	2						
10	6	5				8849.493	1	-3						
10	6	4				8849.343	6	15						
11	0	11				8566.067	12	11	8890.130	3	1			
11	1	11				8566.067	12	16	8891.593	1	-4	8343.825	9	3

TABLE 3—*Continued*

			(300)			(201)			(003)			(121)		
J	K_a	K_c	E	Δ	δ	E	Δ	δ	E	Δ	δ	E	Δ	δ
1			2	3	4	5	6	7	8	9	10	11	12	13
11	1	10				8663.339	2	-9	8990.283	2	0	8458.696	2	- 1
11	2	10				8663.384	7	2	8988.576	0	1			
11	2	9				8745.059	1	1						
11	3	9				8746.470	1	-6						
11	3	8							9127.117	2	-2			
11	4	7							9171.280		-7			
11	5	6				8896.643	2	-2						
11	6	5				8980.473	1	0						
11	6	6				8980.867		5						
12	0	12				8682.214	10	-2	9007.391		-13			
12	1	12				8682.214	10	-13	9007.391		-13			
12	1	11				8789.129	1	4						
12	2	11							9116.417	3	1			
12	2	10				8880.870	2	-6						
12	3	10				8880.898	2	-13						
12	4	9				8960.772	1	0						
12	5	7				9043.980	2	2						
13	0	13				8807.603	7	2						
13	1	13				8807.603	7	-3						
13	1	12				8923.823	2	1						
13	2	11				9025.627		10						
14	0	14				8942.167	4	0						
14	1	14				8942.167	4	-3						
14	1	13				9067.977	3	3						
14	2	13				9067.977	3	-5						

path lengths, we were able to assign transitions belonging to four bands: the abovementioned $2\nu_1 + \nu_3$ band, two other perpendicular-type bands, $3\nu_3$ and $\nu_1 + 2\nu_2 + \nu_3$, and one parallel-type band, $3\nu_1$ (one can find some statistical information concerning studied bands in Table 1). Moreover, some transitions of the $2\nu_2 + 2\nu_3$ band, caused by the strong interaction with the $2\nu_1 + \nu_3$ band, were assigned also.

It is interesting to estimate the relative bandstrengths, which may help in a future more detailed study of the considered bands. To make such estimations, we compared for the bands $3\nu_1$, $2\nu_1 + \nu_3$, $3\nu_3$, and $\nu_1 + 2\nu_2 + \nu_3$ the "pilot" transitions in the R and P branches, $(J+1)_{K'J+1} \leftarrow J_{0J}$ and $(J-1)_{K'J-1} \leftarrow J_{0J}$ with $J = 4$–8 and $K' = 0$ or 1. The result was $I_{3\nu_1}/I_{2\nu_1+\nu_3}/I_{3\nu_3}/I_{\nu_1+2\nu_2+\nu_3} = 1/10$–$18/2$–$3/4$–$7$.

Transitions were assigned on the basis of the known ground state combination differences method and the data from Ref. (*7*) were taken as the ground state rotational energies. In this case, we were able to assign 384 transitions with $J^{\max} = 14$ and $K_a^{\max} = 7$ to the $2\nu_1 + \nu_3$ band ($J^{\max} = 10$, $K_a^{\max} = 6$ and $J^{\max} = 12$, $K_a^{\max} = 5$ in Refs. (*3*) and (*4*), respectively). A small fragment of the spectrum of the $2\nu_1 + \nu_3$ band is illustrated in Fig. 1. One can see strong lines of the $2\nu_1 + \nu_3$ band and, for comparison, one of the weak lines of the $3\nu_1$ band, 7855.1981 cm^{-1}, which is located in this part of the spectrum.

Lines of the other three bands, $3\nu_3$, $\nu_1 + 2\nu_2 + \nu_3$, and $3\nu_1$, are weaker than the corresponding lines of the $2\nu_1 + \nu_3$ band. However, linestrengths belonging to these three bands can increase because of resonance interactions with the $2\nu_1 + \nu_3$ band. For illustration, small fragments of the spectra in the regions of location of the $3\nu_1$, $\nu_1 + 2\nu_2 + \nu_3$, and $3\nu_3$ bands are shown in Figs. 2–4, respectively. We succeeded in assigning 278, 196, and 202 transitions to the $3\nu_3$, $\nu_1 + 2\nu_2 + \nu_3$, and $3\nu_1$ bands, respectively (other statistical information can be found in Table 1). Additionally, six transitions of the $2\nu_2 + 2\nu_3$ band (see Table 2), caused by the strong interaction with the $2\nu_1 + \nu_3$ band, were assigned also.[2]

5. DETERMINATION OF THE HAMILTONIAN PARAMETERS

Line positions obtained at the previous step of analysis were used then for determination of the upper energy levels of the vibrational states (300), (201), (003), and (121). We determined 57, 127, 111, and 62 energies, respectively, which are presented in columns 2, 5, 8, and 11 of Table 3 together with their experimental uncertainties Δ, which are shown in columns 3, 6, 9, and 12, respectively. Obtained energies then were used as the input data in the fit procedure with the Hamiltonian

[2] We were able to assign undoubtedly only six transitions belonging to the $2\nu_2 + 2\nu_3$ band and caused by the strong resonance interaction between the states (022) and (201), mentioned in Section 3. They are listed in Table 2 together with the corresponding obtained values of upper energies.

TABLE 4
Spectroscopic Parameters of the (300), (201), (003), (121), (102), (220), and (022) Vibrational States of the D_2O Molecule (in cm^{-1})[a]

Parameter	(300)	(201)	(003)	(121)	(102)	(220)	(022)
E	7917.675(282)	7916.9196(101)	8203.0816(107)	7672.9334(103)	7987.390(275)	7602.5924(955)	7817.9356(615)
A	14.3544(338)	14.3006(164)	14.0405(163)	17.048606(974)	14.5518(301)	17.4564(108)	16.85793(324)
B	6.95613(697)	7.11270(269)	7.16673(274)	7.312529(330)	7.18660(489)	7.25372(450)	7.29211(694)
C	4.61327(393)	4.61952(306)	4.67317(576)	4.606538(157)	4.74389(553)	4.63327(695)	4.69908(575)
$\Delta_K 10^3$	11.704(185)	8.0771(820)	6.986(109)	16.8047(976)	9.2534721	21.986	21.986
$\Delta_{JK} 10^3$	-1.9823(729)	-1.8753(723)	-0.9110(622)	-1.78489(998)	-1.5232421	-2.368	-2.368
$\Delta_J 10^3$	0.20667(469)	0.29778(360)	0.34529(216)	0.351951(516)	0.30998376	0.3682	0.3682
$\delta_K 10^3$	0.3470859	0.3470859	0.3470859	1.3004	0.3470859	1.3004	1.3004
$\delta_J 10^3$	0.1231099	0.12678(157)	0.1231099	0.14750(236)	0.1231099	0.1531	0.1531
$H_K 10^5$	1.844992	1.844992	1.844992	8.80	1.844992	8.80	8.80
$H_{KJ} 10^5$	- 0.245748	-0.245748	-0.245748	-0.629	- 0.245748	-0.629	-0.629
$H_{JK} 10^5$	- 0.0214969	-0.0214969	-0.0214969		- 0.0214969		
$H_J 10^5$	0.00651382	0.00651382	0.00651382	0.0106	0.00651382	0.0106	0.0106
$h_K 10^5$	0.379064	0.379064	0.379064	1.073	0.379064	1.073	1.073
$h_{JK} 10^5$	- 0.0052887	-0.0052887	-0.0052887		- 0.0052887		
$h_J 10^5$	0.0032263	0.0032263	0.0032263	0.00518	0.0032263	0.00518	0.00518
$L_K 10^7$	-0.596454	-0.596454	-0.596454	-3.02	-0.596454	-3.02	-3.02
$L_{KJK} 10^7$	0.15158	0.15158	0.15158		0.15158		
$L_{KJ} 10^7$	-0.038484	-0.038484	-0.038484		-0.038484		
$L_{JJK} 10^7$	0.0005476	0.0005476	0.0005476		0.0005476		
$L_J 10^7$	-0.00016828	-0.00016828	-0.00016828		-0.00016828		
$l_K 10^7$	-0.17362	-0.17362	-0.17362		-0.17362		
$l_J 10^7$	-0.000083613	-0.000083613	-0.000083613		-0.000083613		
$P_K 10^9$	0.151661	0.151661	0.151661		0.151661		

[a] Values in parentheses are the 1σ statistical confidence intervals. Parameters presented without confidence intervals were fixed to their initial values (see text for details).

discussed in Section 3. In this case, because information about rotational energy structures of the three vibrational states, (220), (022), and (102), of the Hamiltonian [1]–[4] is absent, the problem of the choice of starting values of parameters is very important not only for the "appeared" (201), (003), (121), and (300) states, but for the "dark" ones (220), (022), and (102) as well. In our case, the initial values of the pure vibrational energies E^i, of the Darling–Dennison and Fermi-resonance parameters F_0^{ij}, and of the Coriolis-interaction parameters C_y^{ij} were estimated from the preliminary "global vibrational–rotational fit" of 23 bands belonged to the $v = 0, \frac{1}{2}, 1, 2, \frac{3}{2}, 2, 3, 4$, and 5 poliads. Initial values of all centrifugal distortion coefficients of the (300), (201), (102), and (003) states, on the one hand, and of the (220), (121), and (022) states, on the other hand, were fixed to the values of the corresponding parameters of the ground vibrational state and of the (020) state, respectively, from Ref. (*7*). The initial values of all resonance interaction parameters, except for the abovementioned F_0^{ij} and C_y^{ij} parameters, were equal to zero.

Results of the fit are presented in Tables 4 and 5 and in last three columns of Table 1. As one can see from Table 4, all varied rotational and centrifugal distortion parameters have physically suitable values which correlate both with each other and with rotational and centrifugal distortion parameters of the ground vibrational state from Ref. (*7*). All the values of the resonance interaction parameters in Table 5 also have reasonable order of magnitude. However, we should pay attention to the absence of the $F_0^{201-121}$ parameter in Table 5, in spite of the fact that, in accordance with the general vibration–rotation theory (*6*), it should be far from zero. In fact, this parameter was varied, and its value was determined to be equal to zero as a result of the fit. The obtained "discrepancy" between the general theory and the result of the fit can be understood if one will remember that in our Hamiltonian model we omitted three vibrational state of the poliad, (140), (041), and (060). In principle, the first two of them interact with the (121) vibrational state, and the absence of corresponding interactions in the Hamiltonian model leads to some distortions in kept parameters.

It should be mentioned that the presence of strong resonance interactions between all seven vibrational states considered in this study gave the possibility not only to determined rotational, centrifugal distortion, and resonance interaction parameters of the appeared four bands, $2\nu_1 + \nu_3$, $3\nu_3$, $\nu_1 + 2\nu_2 + \nu_3$, and $3\nu_1$, but also to estimate band centers, rotational, and resonance interaction parameters of the three dark states, (220), (022), and (102), from the fit. In this case, one can see that the confidence intervals for the fitted parameters of the states (220), (022), and (102) are small. From this point, those parameters can be called suitable of the concrete Hamiltonian

TABLE 5
Parameters of Resonance Interactions Between the States of the $v_1 + v_2/2 + v_3 = 3$ Poliad of the D_2O Molecule (in cm^{-1})[a]

Parameter	Value	Parameter	Value	Parameter	Value
		Fermi Type Interactions			
$F_0^{300-102}$	-94.45(104)	$F_K^{300-102}$	0.1968(110)		
$F_0^{300-220}$	20.0	$F_K^{300-220}$	0.4367(228)		
$F_{xyK}^{300-220}10^3$	2.915(184)	$F_{xyJ}^{300-220}10^3$	0.6126(234)	$F_{xyKK}^{300-220}10^5$	-4.948(660)
$F_0^{300-022}$	-4.45(222)				
$F_0^{102-022}$	11.0				
$F_0^{220-022}$	-43.0	$F_{xy}^{220-022}$	0.1014(128)	$F_{xyK}^{220-022}10^3$	-4.200(246)
$F_0^{201-003}$	-72.0	$F_K^{201-003}$	0.2875(321)	$F_{xy}^{201-003}$	-0.06783(570)
		Coriolis Type Interactions			
$C_y^{300-201}$	-1.0138(615)	$C_{yK}^{300-201}10^2$	0.6128(680)	$C_{xz}^{300-201}$	-0.45649(890)
$C_y^{102-201}$	1.894(151)	$C_{yK}^{102-201}10^2$	-0.771(116)	$C_{yJ}^{102-201}10^2$	0.1199(117)
$C_{xzJ}^{102-201}10^3$	0.2695(244)	$C_{yxy}^{102-201}10^2$	-0.02484(245)	$C_{yxyK}^{102-201}10^4$	0.2484(396)
$C_{xzK}^{220-201}10^3$	-1.1178(546)				
$C_y^{022-201}$	-1.1883(645)	$C_{yK}^{022-201}10^2$	2.457(126)		
$C_{xz}^{022-201}10$	-1.3478(817)	$C_{xzK}^{022-201}10^3$	1.999(106)		
$C_y^{102-003}$	-2.958(131)	$C_{yK}^{102-003}10^2$	-0.957(120)	$C_{yKK}^{102-003}10^4$	0.862(152)
$C_{xz}^{102-003}10$	-4.0545(709)	$C_{xzKK}^{102-003}10^5$	0.4946(586)		
$C_{yK}^{300-121}10^2$	1.6447(450)				
$C_y^{220-121}$	-0.8	$C_{yxy}^{220-121}10^2$	-0.17041(726)		
$C_{xz}^{220-121}10$	-4.5308(274)	$C_{xzK}^{220-121}10^3$	5.6497(638)	$C_{xzJ}^{220-121}10^3$	0.1849(379)
$C_y^{022-121}$	-0.8	$C_{yK}^{022-121}10^2$	2.339(328)	$C_{yKK}^{022-121}10^4$	10.495(896)
$C_{xz}^{022-121}10$	-2.332(111)	$C_{xzK}^{022-121}10^3$	-7.146(320)	$C_{xzJK}^{022-121}10^5$	6.189(279)
$C_{yxy}^{022-121}10^2$	0.0870(164)				

[a] See footnote (*a*) to Table 4.

model. However, one should remember that (022), (220), and (102) are the dark states which, in our case, have no real experimentally determined rovibrational energies. In principle, if one will change a Hamiltonian model [e.g., add into consideration resonance interactions with the states (140), (041), and/or (060)], the dark character (e.g., the absence of experi-

mental energy levels) of the states (022), (220), and (102), can lead to some changes of values of the fitted parameters in comparison with the values presented in Table 4. Analysis of analogous situations which were modeled with the appeared bands showed that the fitted parameters of such dark states may be changed to the values (5–10) $\times \sigma$, where σ are the confidence intervals of corresponding dark-state parameters. From this point, the statistical confidence intervals of the abovementioned parameters of the states (022), (220), and (102) from the second part of Table 4 should be considered only as the first approximation. The real σ values should be taken (5–10) times larger.

The values $\delta = E^{\text{exp}} - E^{\text{calc}}$ in columns 4, 7, 10, and 13 of Table 3 illustrate the reproductive power of obtained parameters. They are presented in units of 10^{-3} cm^{-1} (values E^{calc} are the values of rovibrational energies calculated with the parameters of Tables 4 and 5), and one can see satisfactory agreement between experimental and calculated values. This fact can be considered as an additional confirmation of the physical correctness of the obtained parameters (in total, 71 free parameter which were determined from the fit of 359 initial experimental energies). The last three columns of Table 1 present statistical information which illustrates reproductive power of the determined parameters. Column 3 of that table presents, for comparison, results of theoretical predictions of the band centers on the basis of the MORBID method from Ref. (*8*). One can see satisfactory correspondence between both sets of band centers.

6. CONCLUSION

Analysis of the high-resolution Fourier transform spectra of the D_2O first decade was carried out in the framework of the Hamiltonian model which took into account resonance interactions between the seven states, (300), (201), (102), (003), (220), (121), and (022). Assigned from the experimentally recorded spectrum transitions belonged to the four bands, $2\nu_1 + \nu_3$, $3\nu_3$, $\nu_1 + 2\nu_2 + \nu_3$, and $3\nu_1$, gave the possibility both of obtaining rotational, centrifugal distortion, and resonance interaction parameters of appeared states (201), (003), (121), and (300), and of estimating band centers, rotational, and resonance interaction parameters of the three dark states, (220), (022), and (102), from the fit.

ACKNOWLEDGMENTS

This work was supported by Chinese National Science Foundation, Chinese Academic of Sciences, and Chinese Pan-Deng Project. O. Ulenikov thanks University of Science and Technology of China for guest professorship, and G. Onopenko thanks the Ru Jia-xi Foundation for financial support during their staying in Hefei in March–May 2000.

REFERENCES

1. Sheng-gui He, O. N. Ulenikov, G. A. Onopenko, E. S. Bekhtereva, Xiang-huai Wang, Shui-ming Hu, Hai Lin, and Qing-shi Zhu, *J. Mol. Spectrosc.* **200,** 34–39 (2000).
2. Xiang-huai Wang, O. N. Ulenikov, G. A. Onopenko, E. S. Bekhtereva, Sheng-gui He, Shui-ming Hu, Hai Lin, and Qing-shi Zhu, *J. Mol. Spectrosc.* **200,** 25–33 (2000).
3. W. S. Benedict, N. Gailar, and K. Plyler, *J. Chem. Phys.* **24,** 1139–1165 (1956).
4. Y. Cohen, I. Bar, and S. Rosenwaks, *J. Mol. Spectrosc.* **180,** 298–304 (1996).
5. J. K. G. Watson, *J. Chem. Phys.* **46,** 1935–1949 (1967).
6. D. Papousek and M. R. Aliev, "Molecular Vibrational–Rotational Spectra," Elsevier, Amsterdam-Oxford-New York, 1982.
7. N. Papineau, J.-M. Flaud, C. Camy-Peyret, and G. Guelachvili, *J. Mol. Spectrosc.* **87,** 219–232 (1981).
8. Per Jensen, S. A. Tashkun, and Vl. G. Tyuterev, *J. Mol. Spectrosc.* **168,** 271–289 (1994).